Journal of Structural Geology 26 (2004) 1067–1086

JOURNAL OF STRUCTURAL GEOLOGY

www.elsevier.com/locate/jsg

Structural controls on Witwatersrand gold mineralisation

S.J. Jolley[a,b,*], S.R. Freeman[a], A.C. Barnicoat[a,c], G.M. Phillips[a], R.J. Knipe[a], A. Pather[d], N.P.C. Fox[d], D. Strydom[e], M.T.G. Birch[d], I.H.C. Henderson[a,f], T.W. Rowland[d,g]

[a]*Rock Deformation Research Ltd, Earth Sciences, University of Leeds, Leeds LS2 9JT, UK*

[b]*Shell UK Exploration and Production Ltd, 1 Altens Farm Road, Nigg, Aberdeen AB12 3FY, UK*

[c]*CRC Geoscience Australia, PO Box 378, Canberra, ACT 2601, Australia*

[d]*AngloGold, 11 Diagonal Street, Johannesburg 2001, South Africa*

[e]*Anglo-American, 44 Marshall Street, Johannesburg 2001, South Africa*

[f]*Norwegian Geological Survey, Mineral Resources Division, Leiv Eirikssons Vei 39, Lade, Trondheim 7491, Norway*

[g]*Goldfields Limited, 24 St Andrews Road, Parktown, Johannesburg 2193, South Africa*

Received 6 January 2003; received in revised form 16 September 2003; accepted 22 October 2003

Abstract

Structural controls on the distribution of gold in the Witwatersrand Basin can be seen at scales ranging from that of thin sections up to regional seismic data sets. At the thin section scale, gold occurs largely in fractures with hydrocarbons. These fractures are associated with pulses of thrusting deformation that occurred in the latter stages of the basin's development. The distribution of thrust–fracture networks (and therefore gold) is controlled by the mechanical attributes of the host stratigraphy. Thrust displacements are generally very low, with structures exploiting depositional contacts and mesoscale sedimentary bedforms. Many of the small faults are isolated from each other with bimodal vergence between larger-scale thrusts of the same age. Early-formed faults and fractures become folded and faulted by subsequent propagation of larger-scale thrusts. These characteristics are consistent with formation of the mineralised thrust–fracture networks in the frontal, low-displacement parts of a thrust system. In the Carletonville goldfield, the prospectivity of the Ventersdorp Contact Reef (VCR) has been evaluated by using underground observations to pinpoint the structural habitat of gold, and therefore characterise the size of prospective zones around structures intersecting the VCR, mapped within 3D seismic data. In the Welkom goldfield, the controls on gold distribution at the Tshepong mine have been characterised from 3D seismic data, drilling and underground observations, and used to develop an ore-body model that aids reserve estimation and production planning.

Keywords: Thrust; Fracture; Propagation; Mechanical stratigraphy; Hydrothermal gold; Witwatersrand

1. Introduction

Almost 50,000 tonnes or 40% of the gold ever mined has come from the Witwatersrand Basin, which still contains over a third of the world's unmined reserves (Frimmel and Minter, 2002). Extraction of the basin's gold is now in its mature stages, with exploration and production efforts being focused primarily on identifying remaining ore pockets, and larger prizes in down-dip extensions to existing mine infrastructure. The geoscience and engineering aspects of this have become increasingly challenging and geological targeting has become increasingly driven by process models.

The gold deposits have traditionally been considered to have formed by alluvial placer processes, but much recent work has cast doubt upon this idea, and instead advocates a hydrothermal origin for the mineralisation, with syn-kinematic fluid flow controlled largely by structural permeability (e.g. Phillips and Myers, 1989; Barnicoat et al., 1997; Jolley et al., 1999; Phillips and Law, 2000; Fox, 2002). This paper illustrates how structural data gathered at a range of scales from that of thin sections to regional seismic lines can be synthesised to characterise the role of deformation in the hydrothermal processes experienced by the Witwatersrand rocks and presents some examples of the application of structural geology to exploration, ore

* Corresponding author..
E-mail address: steve.jolley@shell.com (S.J. Jolley).

0191-8141/$ - see front matter © 2004 Elsevier Ltd. All rights reserved.
doi:10.1016/j.jsg.2003.11.011

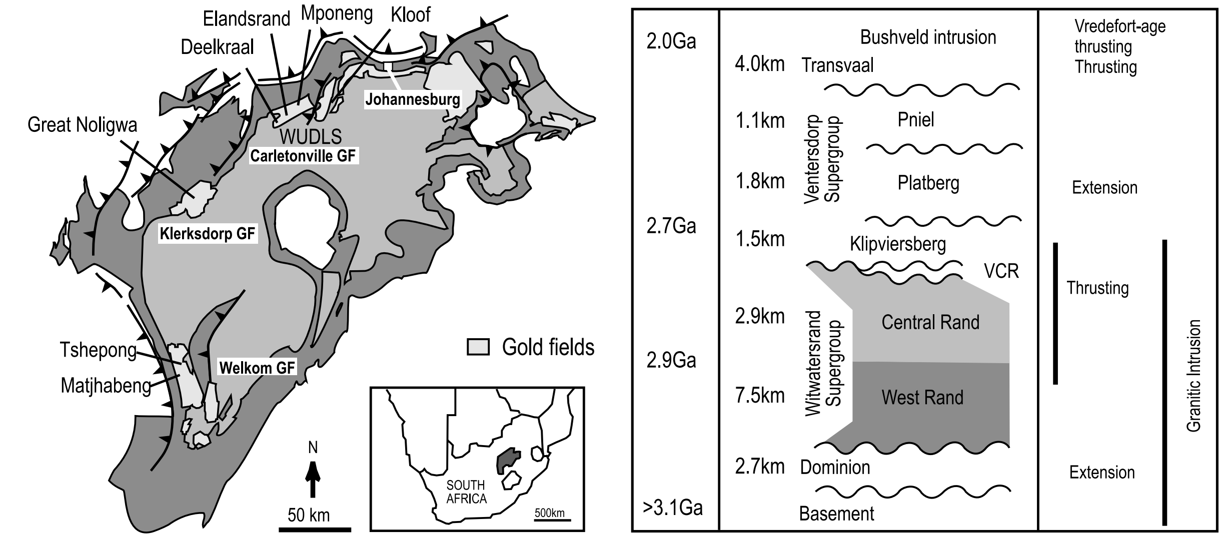

Fig. 1. (a) Simplified geological map of the Witwatersrand Basin, with post-Witwatersrand stratigraphy removed and late-Witwatersrand thrust-related structures shown. The mines and goldfields discussed in the text are indicated. (b) Generalised tectono-stratigraphic framework, with approximate dates and group-level maximum thicknesses seen in the basin, derived from Coward et al. (1995). Note that following a company reorganisation several years ago, some mines were re-named as follows: Great Noligwa (formerly Vaal Reefs 8 shaft); Matjhabeng (Western Holdings); Mponeng (Western Deep Levels South); Tshepong (Freegold 2 shaft).

evaluation and mining of Witwatersrand gold deposits. The ideas presented here are based on a decade of our work, during which we have interpreted regional 2D seismic lines and seven 3D seismic surveys, conducted underground mapping at 12 gold mines, collated countless mine plans, logged at least 30 km of drillcore at centimetre scale, processed nearly a million gold assay data points, and examined several hundred samples and several thousand gold grains by scanning electron microscopy (SEM).

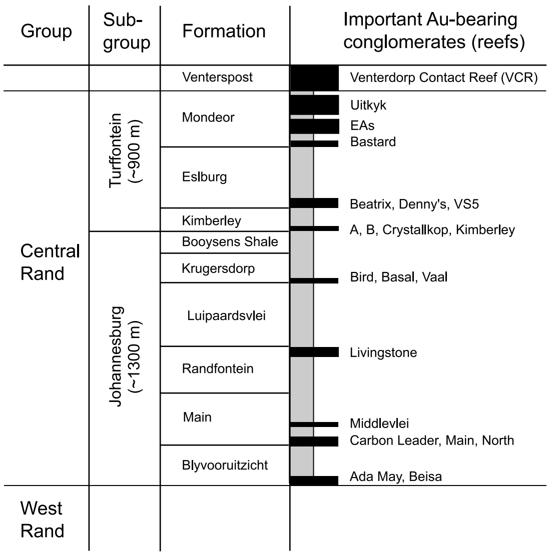

Fig. 2. Stratigraphy of the Central Rand group showing important gold-bearing horizons or 'reefs' (simplified from Frimmel and Minter (2002); megasequence boundaries after Coward et al. (1995)). Sub-group level thicknesses typical of those seen within the goldfields.

1.1. Regional setting

A number of recent papers contain excellent reviews of the complex geology of the Witwatersrand Basin (e g. Coward et al., 1995; Phillips and Law, 2000; Frimmel and Minter, 2002), so only a brief summary is presented here with emphasis on aspects that are important in this paper. The basin is situated on the ancient Kaapvaal craton in South Africa, where it formed in an Andean-style collisional setting during the Archaean. It overlies a basement composed of granitoids and greenstone belts, and ca. 3.1 Ga volcanics and sediments of the Dominion Group (Fig. 1). The Witwatersrand Supergroup, comprises the West Rand Group, which is dominated by foredeep shales and sandstones; and the ca. 2.9–2.7 Ga Central Rand Group, composed largely of alluvial sandstones and auriferous conglomerates, which form major depositional packages with sequence boundaries induced substantially by tectonic activity around the basin, particularly to its north and west (Fig. 2; Coward et al., 1995). Unconformably overlying the Central Rand sediments is the late-Archaean Ventersdorp Supergroup, comprising the ultramafic and mafic lavas of the Klipriviersberg Group, succeeded by the mixed mode volcanics and sediments of the Platberg and Pniel groups, deposited in a successor basin containing grabens and half grabens focused on earlier thrust-related structures. These basins are unconformably overlain by clastic and carbonate sediments of the early Proterozoic Transvaal Supergroup. The composite Witwatersrand basin-fill is now metamorphosed to greenschist facies grade (Phillips, 1987).

1.2. Gold mineralisation

Most of the gold in the Witwatersrand Basin is hosted by

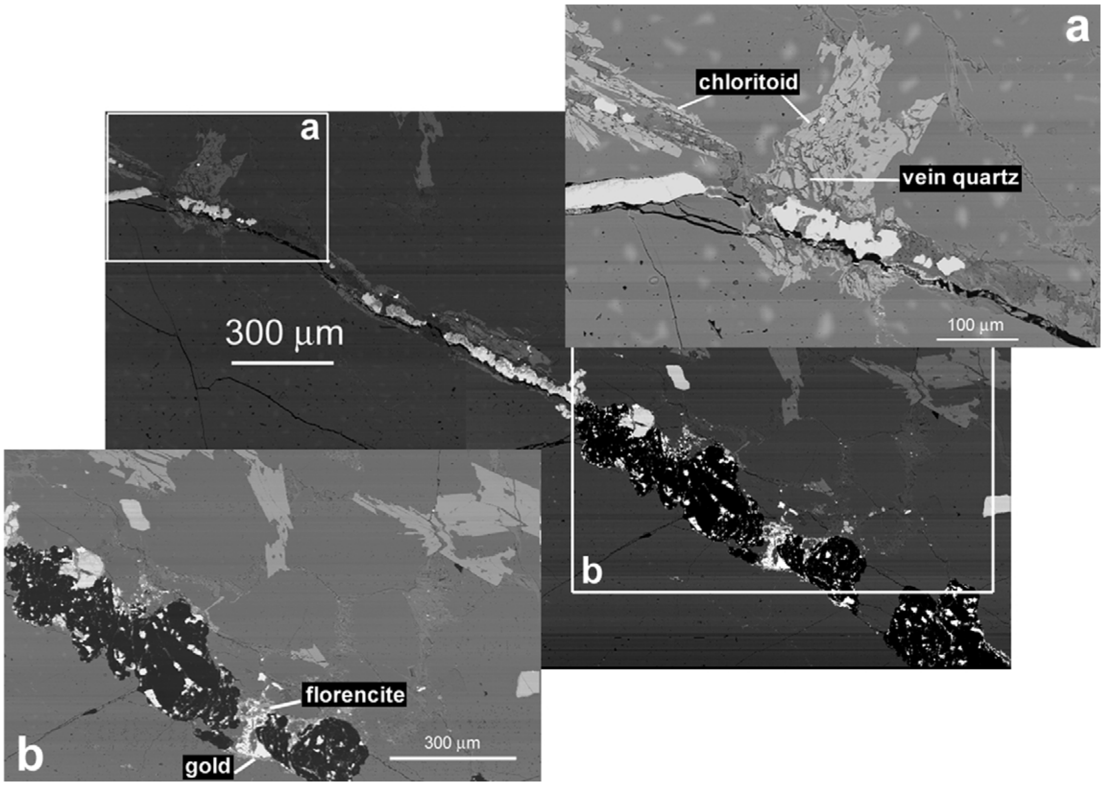

Fig. 3. Back-scattered SEM micrograph showing a fracture containing hydrocarbons (black, with white inclusions of uraninite), pyrrhotite (pale grey) and quartz. Close-ups show matrix comprises quartz and chloritoid (dark grey), with chloritoid cut by a pyrrhotite–quartz assemblage of vein and gold and florencite associated with fracture fill hydrocarbons (black, with white inclusions of uraninite). Carbon Leader Reef.

Central Rand Group conglomeratic layers of varying lithological character, parochially referred to as 'reefs' (Fig. 2). In most cases, the gold is intimately associated with a hydrocarbon (e.g. Parnell, 1996; Gray et al., 1998; England et al., 2001). This hydrocarbon is now a mesophase, formed by the rapid heating and proto-graphitisation of oil derived from within the Witwatersrand basin (Gray et al., 1998; Gize, 2000). The gold ores are found within mineralogically altered stratigraphies, which include highly aluminous rocks (Palmer et al., 1989; Barnicoat et al., 1997; Jolley et al., 1999; Phillips and Law, 2000; Fox, 2002). Mineralogies are dominated by sericite and pyrophyllite with lesser amounts of chloritoid, chlorite and/or sudoite. Whilst some workers still maintain that these assemblages and the associated extreme compositions are the results of weathering and metamorphism rather than metasomatism (e.g. Frimmel and Minter, 2002), the distribution of aluminous parageneses which cross stratigraphy (Barnicoat et al., 1997; Phillips and Law, 2000) together with the compositional data and the occurrence of pure pyrophyllite rocks (Barnicoat et al., 1999) are compelling indicators that post-depositional processes were responsible.

Most workers on the Witwatersrand now acknowledge that most or all of the gold present is paragenetically late (e.g. Feather and Koen, 1975; Barnicoat et al., 1997; Phillips and Law, 2000; England et al., 2001; Frimmel and Minter, 2002). However, interpretations of this observation are still controversial, with some workers (e.g. Minter, 1999; Frimmel and Minter, 2002) contending that the gold was originally detrital and has been remobilised very locally (over distances of millimetres to centimetres). Other workers (e.g. Barnicoat et al., 1997, 1999) contend that the mineralisation is hydrothermal, with gold sourced from either highly disseminated material within the basin or from a source outwith the Witwatersrand sediments, and point to the difficulties of dissolving and then locally reprecipitating gold without evidence of the unreasonably substantial, small-scale gradients in chemistry that would be required.

2. Structural siting of gold

While the gold-bearing horizons are generally conglomeratic, their character varies widely, some being pebble lags whilst others are composed of stacked fluvial channels 1–2 m in thickness. Typically, mineralisation occurs through no more than 1 m of stratigraphy, and in many cases almost all of the gold is contained within 10 cm of the conglomerate, in association with micro- and meso-scale fracture networks, as described below. For example, underground observations and mapping of the Vaal Reef at Great Noligwa mine reveal that small-scale flat-lying structures are widespread. Thin phyllonites often mark the base and

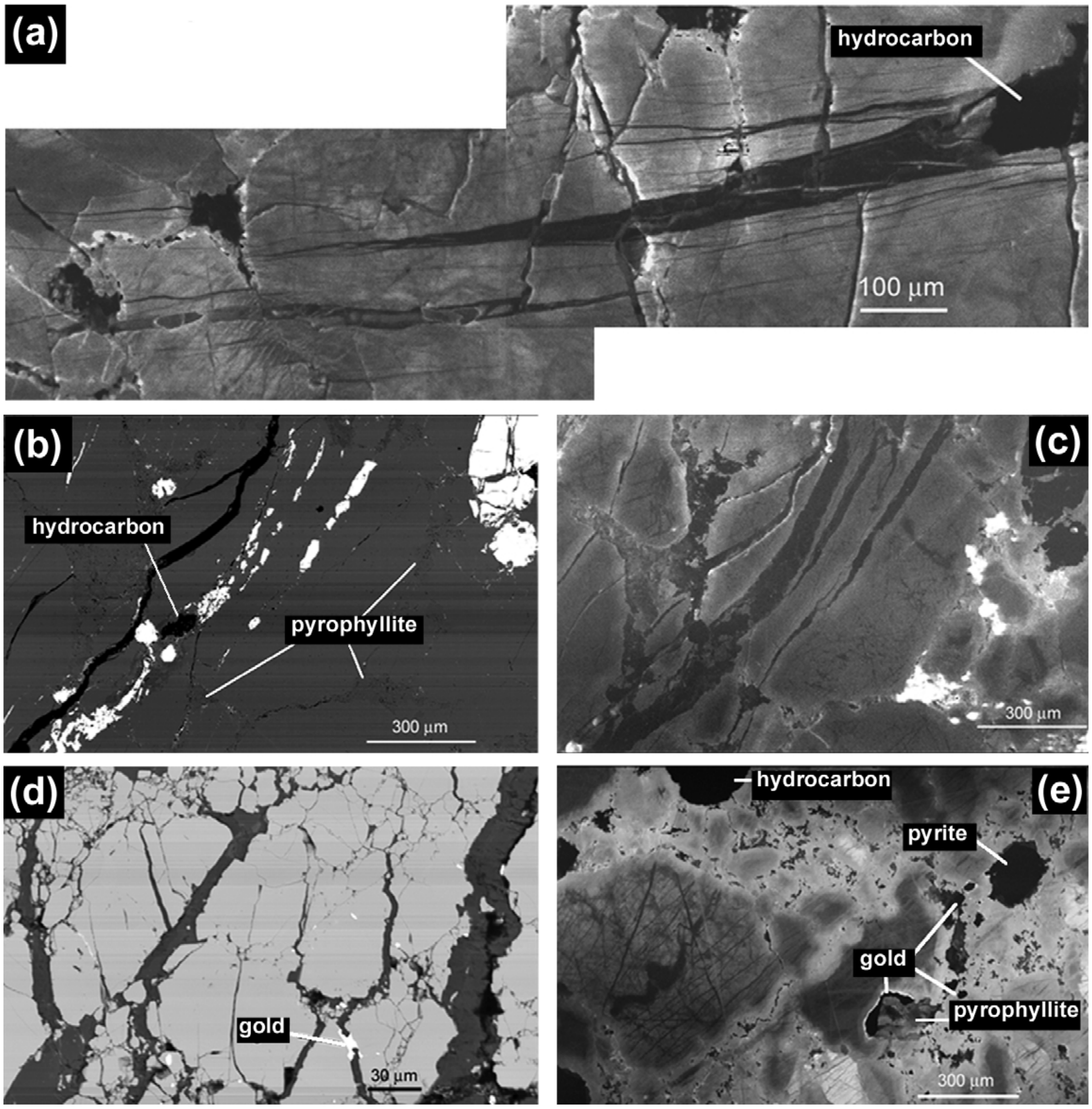

Fig. 4. (a) Cathodoluminescence image of poorly luminescent quartz filling a fracture in a detrital quartz grain accompanied by hydrocarbon 'nosing' along the fracture. Carbon Leader. (b) Back-scattered SEM image showing hydrocarbons and pyrite in a matrix of quartz and pyrophyllite. Note the undeformed nature of the hydrocarbons. Basal Reef, Matjhabeng mine. (c) Cathodoluminescence image of (b) showing the hydrocarbons and elongated pyrite to be contained in quartz cemented fracture. (d) Gold accompanied by pyrophyllite (dark grey) in fractures within pyrite. Basal Reef, Matjhabeng mine. (e) Cathodoluminescence image showing detrital quartz grains with a wide range of luminescence signatures. Gold (black) and pyrophyllite occur in a corrosion embayment in one of the quartz grains. Basal Reef, Matjhabeng mine.

top of the reef, and occur frequently throughout much of the Central Rand stratigraphy, being typically clustered around major unconformities intersected in drill core. These fault rocks are generally sub-parallel to stratigraphy, but in detail they often exploit bedforms. Displacements are often very small (centimetre-scale), and since the phyllonites are extremely rich in phyllosilicates, care has to be taken to distinguish them from argillaceous lithologies. However, their local discordance to bedding allows unequivocal interpretation. Zones of sub-horizontal fractures that are locally in mutual cross-cutting relation to the fault rocks are abundant too, often towards the base of the conglomeratic package of the reef but also found at its top and within it. These fractures frequently contain hydrocarbons, but may also be obviously mineralised with sulphides and gold.

We have conducted detailed sedimentological and structural face mapping and gold-assay sampling of the reef packages in 12 gold mines. Despite the practical difficulties experienced in face-mapping fracture networks in challenging underground conditions, this work shows that high gold grades depart from the channelised morphology of the reef lithologies, and instead preferentially follow the smoother profile of thrust-fracture systems exposed in the faces. Indeed, mineralisation is observed in many mines within a variety of sediments outwith the reef package, and even within the Klipriviersberg lavas in the presence of mesoscale thrusts and fractures. These can show relatively

Table 1
Comparison of deformation and gold distribution at Elandsrand and Mponeng

	Elandsrand	Mponeng
Geometries and styles	Linked arrays of forethrusts, backthrusts and underthrusts; footwall plucking; implosion breccias; buttressing.	Similar thrust geometries though linkages less well developed; rare footwall plucking and buttressing.
Thrust displacements	Typically 1–10 m, some 30–50 m, exceptionally up to 100 m.	Most 1–2 m, many 2–5 m, exceptionally over 10 m.
Thrust transport	SSE directed, derived from lineations and gross thrust geometries.	Some SSE trending lineations seen, gross thrust geometries agree.
Thrust imbricate map patterns	Three parallel NE/SW ~800-m-wide thin-skinned imbricate zones inter-linked by NNW/SSE thicker-skinned lateral ramps.	Reticulated ~100–300-m-wide imbricate zones, with linked NE/SW frontal and NW/SE lateral to oblique zones.
Deformation focus	Lava/VCR contact focuses thrust-related deformation; fracture strains focused by thrust ramps and detail of VCR topography and internal stratigraphy.	Lava/VCR contact focuses thrust-related deformation; VCR more complex erosional–depositional architecture, therefore greater focus of fracture strains at VCR topography and internal stratigraphy.
Stope-scale gold distribution	Elevated gold grade coincident with linked thrust imbricates, thrust deformation features and ultracataclasites.	Elevated gold grades coincide with distribution of linked fault zones and ultracataclasites.

high grades equivalent to the reef when sampled for assay, supporting the contention that the fractures carry the bulk of the gold in Witwatersrand orebodies described here.

Our related petrographic work clearly shows that gold is most commonly found intimately associated with meso-phased hydrocarbons within fracture networks in the reef packages (Fig. 3). These fractures also contain pyrrhotite and pyrite with minor amounts of galena, gersdorffite, and brannerite, together with kaolin and quartz. In detail, these fractures post-date alteration characterised by pyrophyllite and chloritoid (Fig. 3). Careful examination reveals that hydrocarbons can be seen both 'nosing' into fractures (Fig. 4a) now filled with authigenic quartz, and in some cases entirely contained, undeformed, within the silicate fracture fill (Fig. 4b and c). This implies that the hydrocarbons were mobile at the time the fractures were open. This contrasts with the interpretation of England et al. (2001) who contend that fracturing occurred after all the hydrocarbon was emplaced. Gold also occurs within fractures in pyrite and in dissolution sites in quartz grains (Fig. 4d and e). Thus, gold displays authigenic morphologies, although Minter (1999) interpreted a few grains to have detrital morphologies when examined in polished sections and liberated by silicate dissolution from a mineralised Basal Reef sample. However, SEM examination of the detailed in situ context of the gold grains in a portion of the same sample shows that the 'peened' morphologies interpreted by Minter (1999) result from delicate marginal intergrowths with florencite–crandallite group minerals that also occur in post-diagenetic fractures; whilst other gold grains in the sample are cemented into post-diagenetic dissolution pits in primary quartz grains (Barnicoat et al., 2000). These gold grains, in common with all others we have observed with clear textural relationships (see also Barnicoat et al., 1997; Jolley et al., 1999), occur in post-diagenetic sites that were not present at the time of sedimentation.

3. Structure and mineralisation, Ventersdorp Contact Reef (VCR), Carletonville goldfield

3.1. Sedimentological framework of the VCR

The Ventersdorp Contact Reef (VCR) refers to the gold bearing conglomeratic portion of the Venterspost Conglomerate Formation, the thin (metre-scale) depositional remnant of a degrading fluvial system that overlies Witwatersrand strata with varying unconformity (Figs. 1 and 2). The VCR therefore has a distinctive pre-deformation geometry, controlled by erosional channels that have left remnant terraces of older VCR conglomeratic packages perched at higher palaeo-topographic levels. The terraces and channels are connected by conglomeratic slopes along which the VCR is thinned or removed (Germs and Schweitzer, 1994; Henning et al., 1994; McWha, 1994). The VCR at Mponeng mine is typically 1–2 m thick and contains coarse

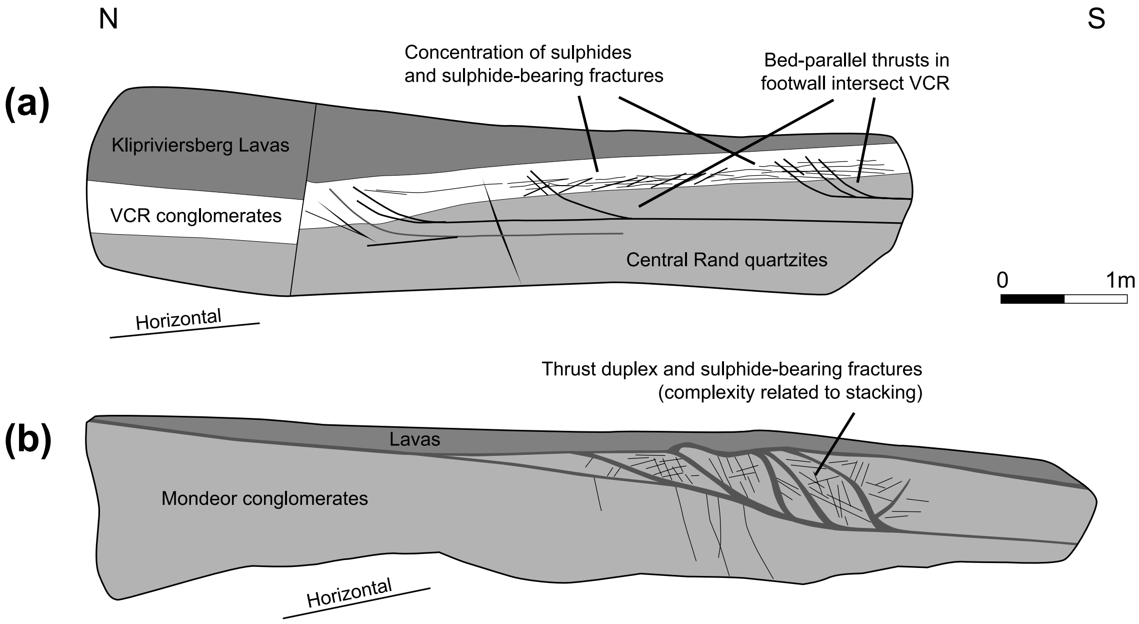

Fig. 5. Mapping of geological features exposed in underground stope faces. (a) Thin VCR conglomerates overlying argillaceous quartzites that sub-crop against the reef. The VCR is preferentially fractured and mineralised where low displacement thrusts within the plane of footwall bedding intersect the reef. Raise tunnel 92/34, Elandsrand mine. (b) Meso-scale duplex and associated mineralised fractures (note fracture complexity related to imbrication). Host 'reef' here is the Mondeor conglomerate package, some distance to the west of the VCR sub-crop against the Klipriviersberg. This is important because the ca. 1-m-thick zone of mineralisation immediately below the lavas is continuous from the VCR into rocks that are normally sterile beneath it. Stope 33/24, Deelkraal mine.

conglomerates and quartzite interbeds preserved within a marked palaeotopography, with local metre-scale slope-terrace relief. To the west, the VCR at Elandsrand mine is thinner and finer-grained with fewer quartzites, and is characterised by less palaeotopography and less angular unconformity with underlying Central Rand rocks. The overlying Klipriviersberg Group lavas were extruded directly onto this regional landform, at first exploiting the channel systems so that basal flows entrain pebbles and interdigitate with VCR sediments (Hall, 1994), and then flooding across the interfluves to rapidly fill the basin.

3.2. Meso-scale structure at Elandsrand and Mponeng mines

At Elandsrand, the VCR has undergone widespread disruption by shallow trajectory mesoscale thrust faults that lie concentrated within or sub-parallel to the plane of the reef, where they constitute a decoupling surface between the Witwatersrand sediments and Klipriviersberg lavas. Local thrust vergence and shear sense reversals are common, as are complex piggyback and break-back thrust sequences. The thrust imbricates typically carry 1–10 m NNW/SSE displacement and occasionally several tens of metres, and are intimately linked to formation of both steep and sub-horizontal gold-bearing fractures, during flexural shear of the reef and short-cutting of ramps (Jolley et al., 1999). Fracturing is also focused by the detail of reef architecture, by slippage across quartzite packages within the dominantly conglomeratic reef, and local buttressing and dilation strains in the reef caused by movement of the rigid lavas against palaeotopography at the VCR/lava contact.

Similar thrust structures are seen 5–6 km to the east at Mponeng, although these have lower displacements and generally simpler less-evolved mesoscale geometries. The thrusts often form isolated structures, and where linked to form arrays they have ramp-flat geometries, a NNW/SSE to NW/SE transport direction and typically several metres of displacement, rarely exceeding 10 m. Many of the thrusts have convex-up 'underthrust' geometries composed of hanging wall ramps in contact with long footwall flats, which detach from the lava/VCR contact with fault-bend-folding restricted to the footwall. Similar structures were seen at Deelkraal mine and have

Fig. 6. (a) Back-scattered SEM micrograph of gold with sulphides in fractures within crushed pyrite host. Thrust–fracture zones in Mondeor conglomerates to the west of the VCR sub-crop, Deelkraal mine. (b) Back-scattered SEM image showing gold with arsenopyrite and brannerite in sub-horizontal fracture within earlier formed sub-horizontal fracture-fill pyrrhotite. VCR, Mponeng mine. (c) Back-scattered SEM image of gold with hydrocarbon and pyrrhotite in complex intersection zone between a steep fracture and a horizontal fracture. VCR, Mponeng mine. (d) Gold with pyrrhotite, epidote and allanite in a matrix corrosion space. VCR, Mponeng mine. (e) Cathodoluminescence image showing gold concentrated within and adjacent to a sub-horizontal fracture. VCR, Mponeng mine.

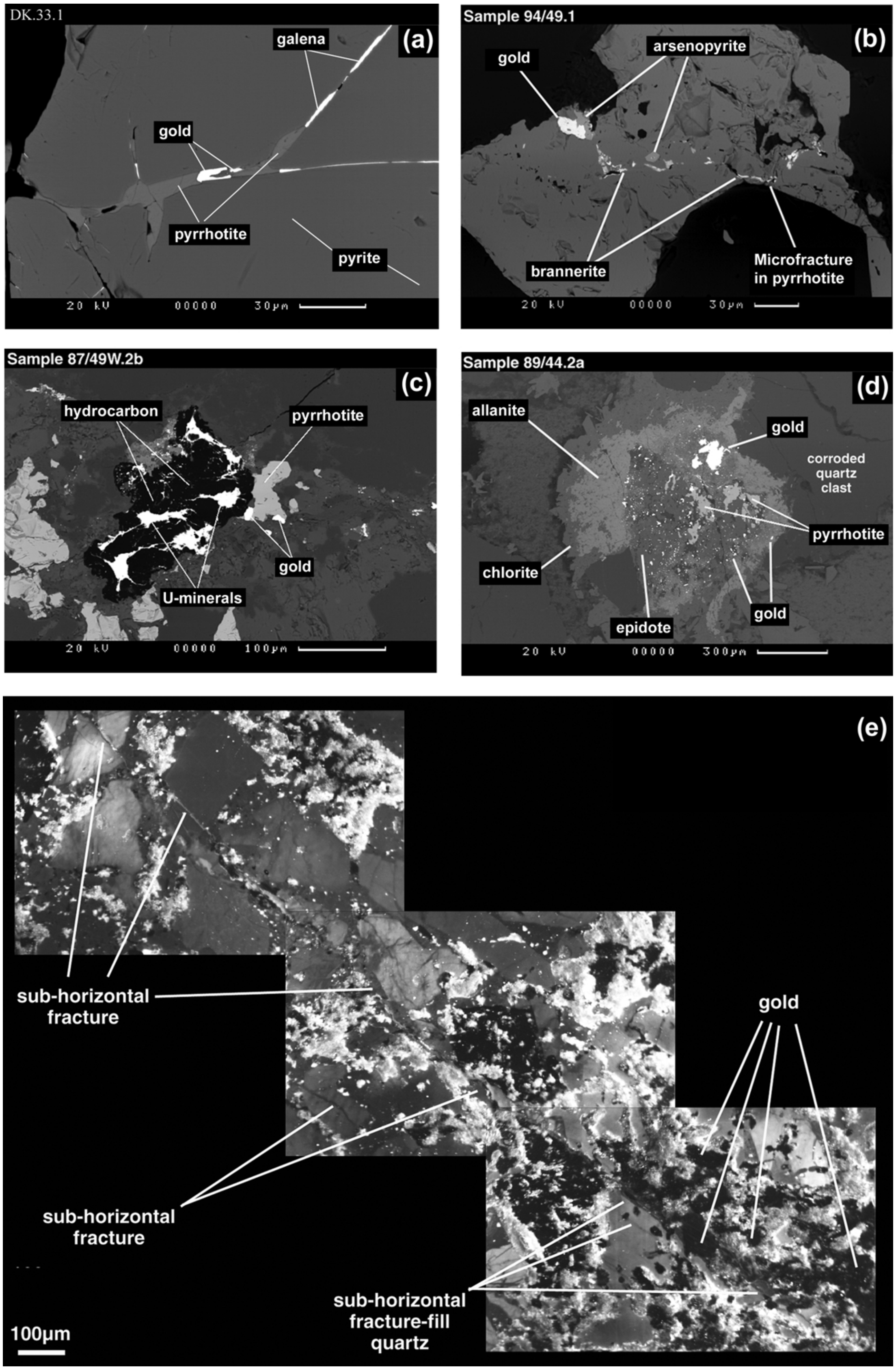
DK.33.1
(a)
galena
gold
pyrrhotite
pyrite
20 kV 00000 30μm
Sample 94/49.1
(b)
gold
arsenopyrite
brannerite
Microfracture
in pyrrhotite
20 kV 00000 30μm
Sample 87/49W.2b
(c)
hydrocarbon
pyrrhotite
gold
U-minerals
20 kV 00000 100μm
Sample 89/44.2a
(d)
allanite
gold
corroded
quartz
clast
pyrrhotite
chlorite
epidote
gold
20 kV 00000 300μm
(e)
sub-horizontal
fracture
gold
sub-horizontal
fracture
sub-horizontal
fracture-fill
quartz
100μm

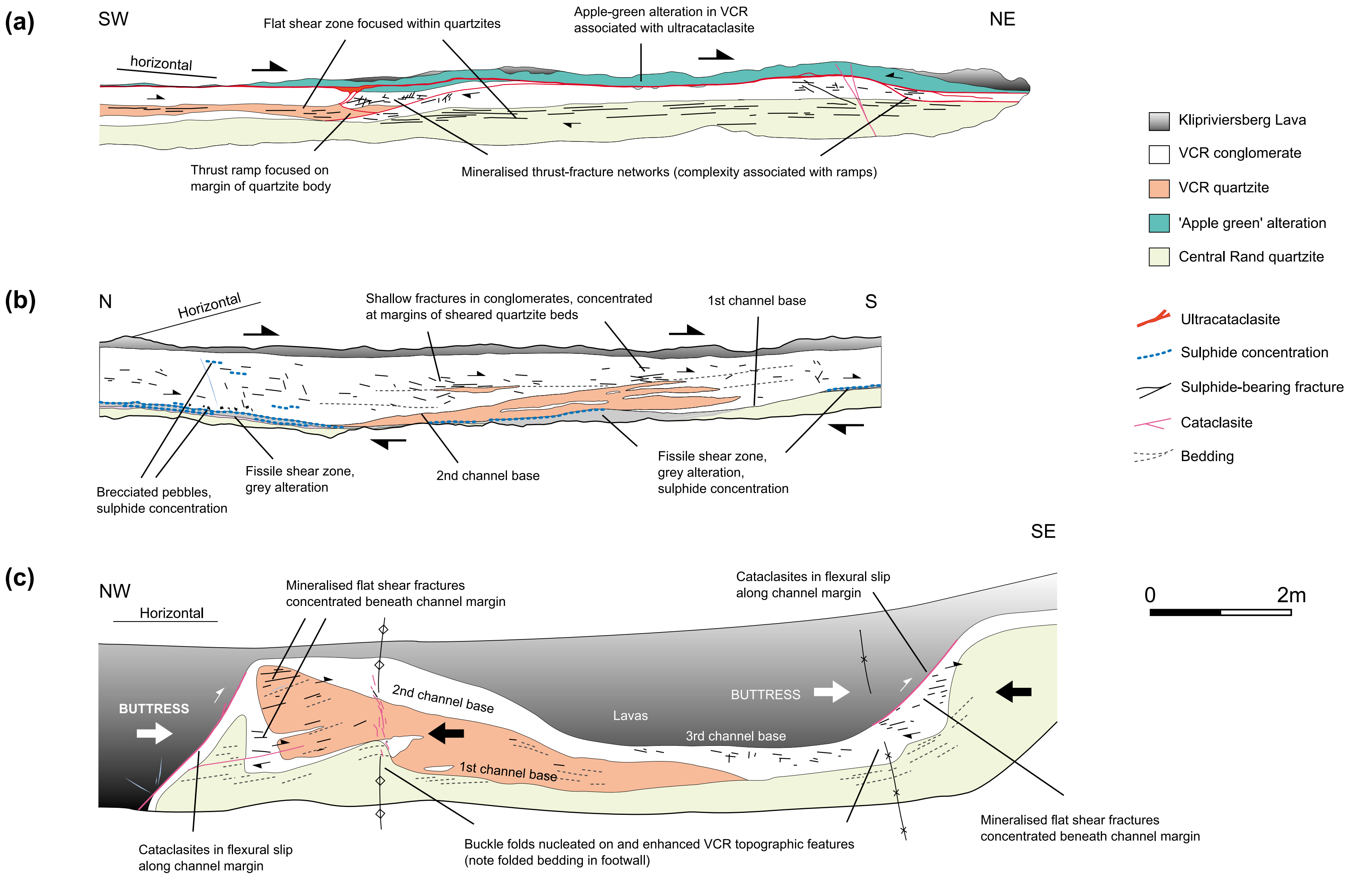

Fig. 7. Geological mapping of mining (stope) faces—measured gold grades quoted here are mine survey average assay results for each stope face illustrated. (a) Structure in VCR terrace facies within an imbricate zone (gold grade 3000 cmg/t). VCR internal stratigraphy part-utilised by thrust structures, and early steep mineralised fractures are cut by later buttressing-related shallow mineralised fractures in thrust ramp. Note slip vector very oblique to face mapped here. Elsberg quartzite footwall. Stope 87/49-W2, Mponeng mine. (b) Typical 1-m-thick terrace facies VCR with conglomerate–quartzite banding onlapping minor channel edges. Approximately 100 m from nearest imbricate zone, but adjacent mining shows ultracataclasites within the footwall quartzites beneath the reef (gold grade 1500 cmg/t). Small early steep and horizontal fractures distributed within the reef, but note shallow structures are concentrated close to sheared thin quartzite beds within the conglomerates. Note slip vector very oblique to face mapped here. Mid-Kimberley argillaceous quartzites in footwall. Stope 84/61-E3, Mponeng mine. (c) Small shallow fracture systems approximately 150 m south of nearest imbricate zone, ultracataclasites not known locally (gold grade 360 cmg/t). Fractures, flexural slip and buckle folding associated with buttressing of base lavas erosional topography against a coincident VCR channel margin. Buckle folding focused on the depositional architecture here absorbs much of the strain. Note slip vector sub-parallel to face mapped here. Mid-Kimberley argillaceous quartzites in footwall. Reef drive tunnel 89/63-RDE, Mponeng mine.

been documented at Elandsrand (Jolley et al., 1999) and Kloof (e.g. Berlenbach, 1995), indicating thrust shortening of the sedimentary package beneath the more rigid lavas is a characteristic structural style in the region. Table 1 provides a comparison of deformation between Elandsrand and Mponeng.

3.3. Mineralised fractures

Several types of gold-bearing fractures formed in association with the thrusting at Mponeng: steep quartz/sulphide-bearing fractures; and sub-horizontal quartz- and/or sulphide-bearing fractures. Both sets of fractures formed in the reef after pervasive matrix alteration, and both sets of fractures host the gold mineralisation. Mine-scale mapping, detailed meso-scale stope face mapping and microstructural observations show that gold grades are greatly elevated above background values where thrust-related deformation features are present at Mponeng. Similarly at Elandsrand, mineralisation is concentrated in the reef where thrusts intersect it (Fig. 5a), and gold grades are an order of magnitude higher where thrust-related fractures are present and mappable. Indeed at Deelkraal mine, which straddles the stratigraphic subcrop of the VCR against the base Klipriviersberg lavas to the west, the older Mondeor conglomerate package lies in contact with the lavas and hosts the mineralisation (Fig. 5b). This is important because the 1–2 m thick zone of gold mineralisation is generally restricted to the VCR, but at Deelkraal the mineralisation is clearly continuous across the VCR subcrop into rocks that are normally sterile beneath it. Mineralisation is therefore clearly associated with the tectonised plane of the base Klipriviersberg, where the lavas lie in contact with a suitably fracture-prone conglomeratic host, and is not particularly restricted to any given depositional unit, thus demonstrating an essentially strata-bound rather than stratiform nature. All of the gold grains we have observed by SEM in VCR samples occur within fractures and fracture intersections, or in matrix corrosion sites within several 100 μm of intersections between fracture edges and the adjacent matrix (Fig. 6; also Barnicoat et al., 1997, fig. 3c; Jolley et al., 1999, fig. 4). Gold is preferentially concentrated in the sub-horizontal fractures, although gold and hydrocarbons also fill steep fractures. These observations demonstrate the broad contemporaneity of the different fracture sets, and the syn-kinematic nature of gold precipitation.

3.4. Relationship between thrusting and mineralised fractures

At Elandsrand, thrust-fracture networks evolved progressively in the reef, due to concentration of thrust-related strains towards the lava/VCR contact (Jolley et al., 1999). Local strain histories began with early layer-parallel shear-driven mineralised fracture formation in the reef interval: first flat fractures focused by the reef's palaeotopography and internal stratigraphy, and then steep fractures caused by broader shearing of the reef and thrust loading. This layer-parallel shear was superceded towards the end of the strain cycle by propagation of thrust imbricates with additional shallow fracture development in ramp segments.

Compared with the VCR at Elandsrand, the VCR at Mponeng is generally thicker, with more pronounced palaeo-topography of perched alluvial terraces and interconnecting slopes at its top, and a more pronounced erosional topography at its base; and the reef's internal stratigraphy of channels, quartzites and coarse units is also more complex. This appears to have restricted thrust propagation along the top of the reef and consequent decoupling of the lavas from the sediments. However, it has provided a stronger focus of fracture strains along the reef's internal stratigraphy (Fig. 7a and b) and against channel margins and topographic edges where indentation and buttressing by the more rigid lavas caused buckle-fold tightening of channels and slope–terrace inflexions and associated fracture formation (Fig. 7c). The thrust–fracture network at Mponeng was therefore initiated by a combination of layer-parallel shear of the VCR package and shortening across VCR topographic features, similar to Elandsrand, although the subsequent propagation of thrust imbricates is less well developed. Where the latter are present, the later-formed shallow fracture sets can be seen in the reef, invariably focused within thrust ramps, and interpreted to result from buttressing and fault short-cut development, similar to examples more commonly seen at Elandsrand.

In detail, the thrust-related fault rocks at Mponeng, in common with those at Elandsrand, initiated as cataclastic zones with quartz cements. These zones were subsequently the focus of significant syn-kinematic fluid flow and hydrothermal alteration, corrosion of quartz and extensive precipitation of phyllosilicates. These cataclasites contain extremely small clasts, and are identical in fabric and evolution to the micaceous ultracataclasites described from Elandsrand, where microstructural data demonstrates that these fault-rocks formed coevally with mineralised fracture systems (Jolley et al., 1999, fig. 4). The key observations are that the ultracataclasites and the fracture fills share a common mineralogy and textural sequence; the two dominant fracture sets display mutual cross-cutting relationships with the fault-rocks; and jogs in fractures host ultracataclasite, whilst the faults tip-out as mineralised fractures such that ultracataclasite is transitional with fracture-fill within a single structure.

Shallowly dipping fractures are more common than steep fractures in the Mponeng VCR. However, mutual cross-cutting relationships are developed between the fractures and between the fractures and the cataclastic fault-rocks, indicating that the fractures formed immediately prior to and during thrust imbrication of the reef. The fracture fill mineralogy is typical of the type associated

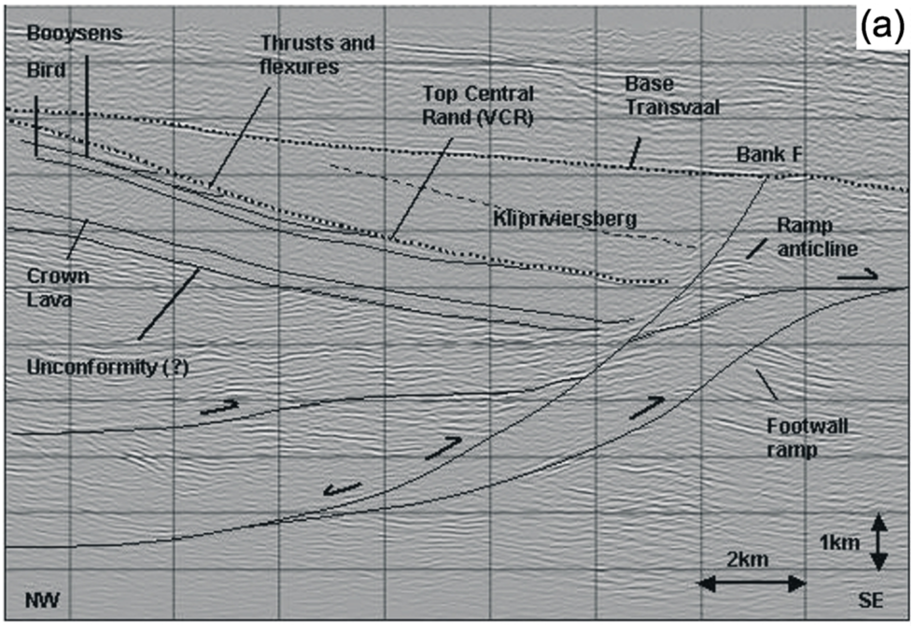

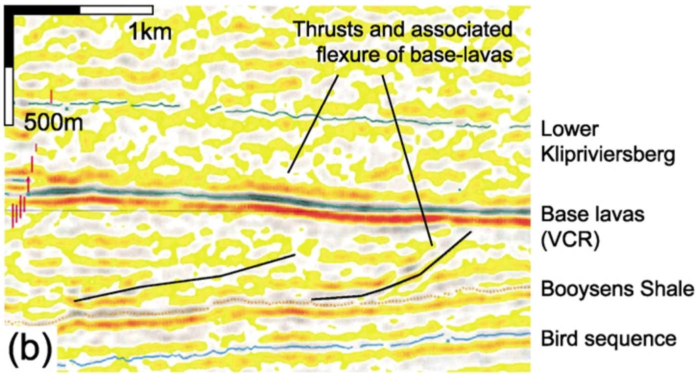

Fig. 8. Cross-sections through the WUDLS 3D seismic survey. (a) Regional section. Thinning and sub-cropping of Central Rand stratigraphy beneath the VCR towards the Bank fault, caused by syn-Central Rand reverse movement on the Bank thrust. Subsequent thickening of the upper Klipriviersberg lavas in the same direction, due to extensional reactivation of the fault. Note downward-facing of thrust detachments (e.g. Booysens Shale), induced by regional tilting during the upper Klipriviersberg to Platberg extension. The section also shows a much earlier angular unconformity in the West Rand, associated with movement on the Bank thrust. (b) Detail (modified from Gibson et al. (2000)), showing thrust climbing from detachment in the Booysens Shale to the base of the Klipriviersberg lavas—note the flexure of the base of the lavas associated with the thrusts.

with mineralisation described above (see also Barnicoat et al., 1997), and is found to include gold grains, indicating that these thrust-related fractures are contemporaneous with mineralisation. The implication is that mineralisation post-dated diagenetic occlusion of sedimentary permeability, and was coeval with and focused by the development of the thrust-fracture networks in the reef; and that gold was precipitated as a consequence of fluid introduction coeval with development of the fault-rocks.

3.5. Mine-scale structure of the VCR in the Carletonville goldfield

The VCR in the Carletonville region alone represents an orebody that is continuous for at least 450 km^2. Whilst individual mines are in the order of 5–10 km across, typically only those areas close to zones of active mining are accessible for direct observation and sample collection. However, mine plans represent a huge data source that contains the detailed data and mappings collected by mine geologists on advancing stope faces during decades of mining activity. We have collated data from these worked-out areas of the mines, supplemented by our own underground observations and SEM work, to build detailed structural models of the gold deposits. An additional source of increasing importance in Witwatersrand mines, is 3D seismic reflection data. Interpretation of this data has been of immense value in determining geological structure in

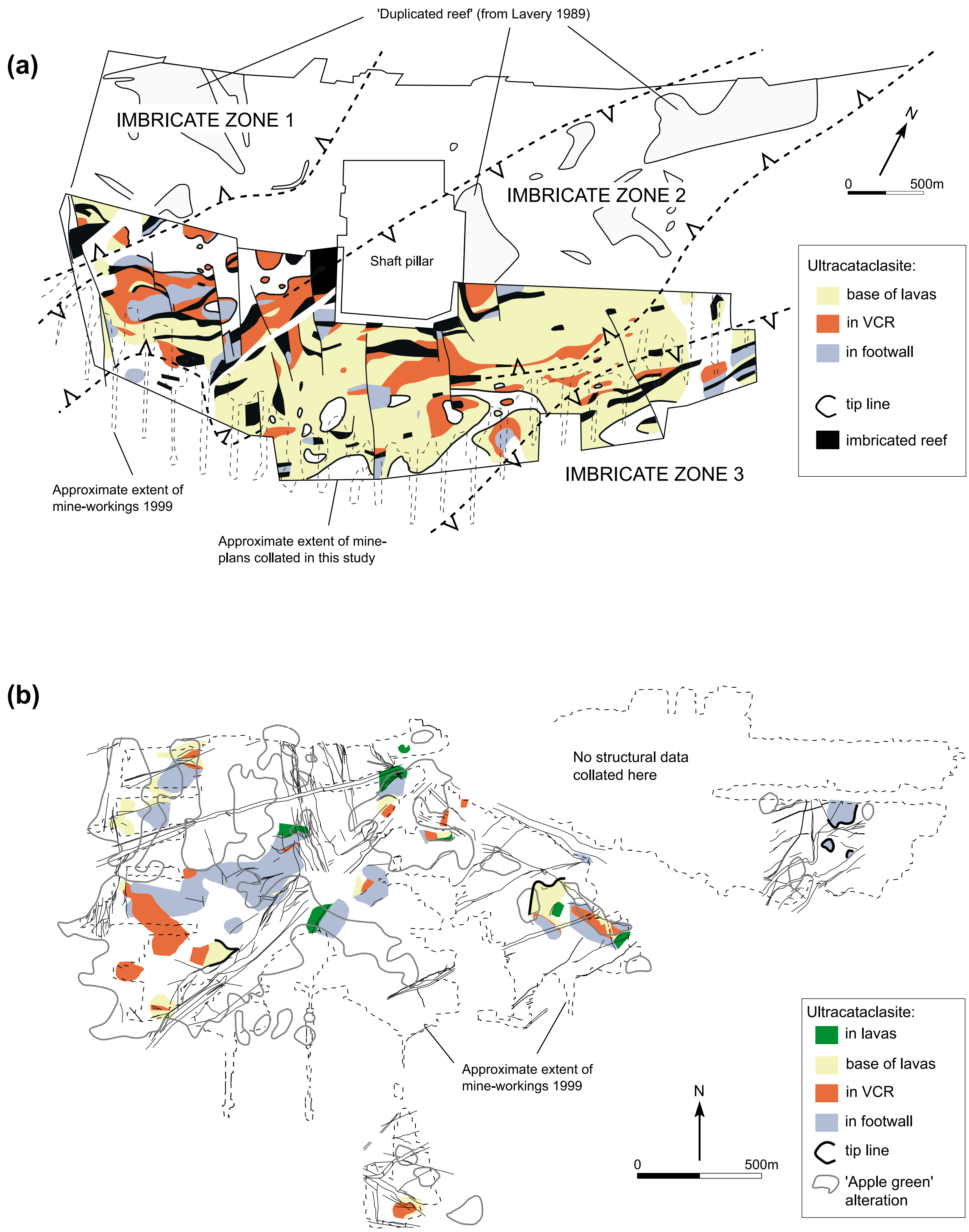

Fig. 9. Structural maps of the VCR at (a) Elandsrand (southern half of map from this work, northern half after Lavery (1989)) and (b) Mponeng mines, compiled from 1:200 mine plans containing underground mappings by mine geologists. Density of mapped faces in the mine plans diminishes in both mines towards the SE, due to changes in work practice. Note three imbricate zones at Elandsrand. These climb section towards the south with trailing imbrication and propagation accomplished through coalescent capture of isolated slip patches. Distribution of thrusting deformation and the 'apple green' alteration at Mponeng shows strong spatial correlation.

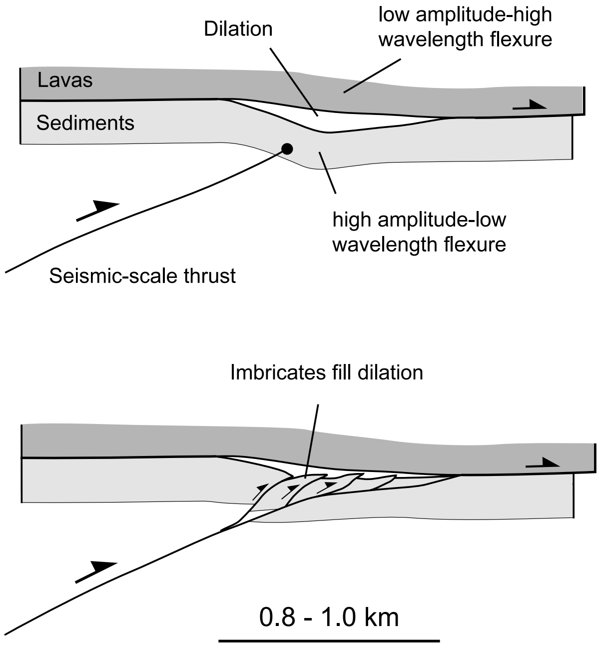

Fig. 10. Cartoon illustrating effects on thrust propagation of differing mechanical stratigraphy. Seismic-scale thrust detaching from Booysens Shale, drives long wavelength–low amplitude flexures in basal lavas, whilst sediments underneath deform with high amplitude–short wavelength structures (e.g. mesoscale imbricate zones). These imbricates close up consequent dilation within the decoupled contact zone.

unmined areas, particularly since the resolution of modern vibroseis surveys allows identification of faults down to a few metres of throw (e.g. Gibson et al., 2000; Stuart et al., 2000).

The structure of the VCR is especially well imaged by 3D seismic data, since it coincides with the substantial acoustic impedance contrast between quartzitic sediments and mafic–ultramafic lavas at the base of the Klipriviersberg Group (e.g. Stuart et al., 2000). Seismically imaged thrusts detach from Witwatersrand strata such as the Booysens Shale (which hosts banded phyllonites and intrafolial folds), and branch into the overlying base lava contact (Fig. 8; Gibson et al., 2000). Here they cause kilometre-scale wavelength, low amplitude (decometre-scale) flexures in the base lavas, and bifurcate to form the mesoscale thrust imbricate zones seen in the Witwatersrand and VCR sediments. These imbricates and fault rocks, which control gold distribution in the VCR, have been mapped by mine geologists and recorded on 1:200 plans. Collation of data from the plans shows that the faults are isolated structures and linked imbricate zones (approximately 800–1000 m wide with 250–300 m total displacement within the VCR at Elandsrand; Fig. 9a). They have similar geometrical characteristics to structures seen in Phanerozoic thrust belts. The main elements are broadly NE/SW-trending imbricates with NNW/SSE transport direction; and NNW/SSE trending steep lateral faults, which in some cases cut deeply enough to connect underlying and overlying imbricate zones.

The NNE/SSW to ENE/WSW trending imbricate zones show clear thrust vergence reversals, style changes and displacement variations across the NNW/SSE trending steep lateral fault systems. Thrusting is towards the SSE, and in general, the thrust-related deformation climbs stratigraphy from the footwall to the top of the reef and in places into the lavas in that direction. The key areas of mapped thrust duplication tend to lie within the 'trailing' (northern) half of the imbricate zones. Both the leading and trailing edges of the thrust zones have lobate margins, with small outlying isolated elliptical thrust faults in the order of 25–50 or 100–150 m across. The NNW/SSE striking lateral fault zones extend beyond the limits of the imbricate zones and have a marked stepping effect on the position of thrusting deformation, indicating linkage to the larger underlying seismic-scale thrusts.

Thrusts at Mponeng are much lower displacement structures than their counterparts at Elandsrand, being typically several metres and rarely more than 10 m. These structures also have a broadly NW/SE transport direction, and when mine plans are collated, they form a pronounced reticulated map pattern composed of steep transport-parallel lateral faults and oblique to frontal zones of shallower dipping imbricates (Fig. 9b). This map shows a clear link between zones of NNE/SSW to E/W trending thrust imbricates and NW/SE trending steep lateral fault systems, and preservation of small isolated thrust structures, particularly in the east of the mine where Booysens Shale underlies the reef.

4. Exploration model for the Carletonville goldfield

4.1. Key controls on gold mineralisation

Gold mineralisation in the VCR is controlled and hosted by Lower Klipriviersberg age thrust–fracture systems (Jolley et al., 1999; Gibson et al., 2000). The detailed nature of fracture formation and hence fluid flow and mineralisation varies regionally across the VCR because of changes in stratigraphy sub-cropping beneath it, the nature of the VCR package and the size and geometry of thrusting. The key controls are as follows.

At regional scale, the interface between rigid lavas and underlying less-competent quartzitic lithologies of the VCR and Central Rand, focuses shear strains and mesoscale imbrication in response to propagation of 'seismic-scale' thrusts towards the contact (Fig. 8). This deformation decouples the lavas from the sediments, thereby partitioning structures of different amplitude and wavelength character developed on either side of the contact and acting to close the consequent dilation that would otherwise occur across the contact, expressed as implosion breccias in some areas of Elandsrand (Fig. 10). At sub-regional scale, the pattern of thrust displacements is seen to decrease to the SE across the mines, in association with the leading edge of the propagating thrust system. Furthermore, thrusting deformation detaching from the Booysens Shale in the NW of the region is terminated where these shales sub-crop against the VCR along the eastern edge of Mponeng. Thrusts detaching along lower parts of the Central Rand stratigraphy such as the Bird sequence, become relevant east of a strain shadow zone immediately below the Booysens Shale (Fig. 8; Gibson et al., 2000). Mine-scale variations in Central Rand lithologies that sub-crop beneath the VCR become significant. For example, thinly bedded or argillaceous quartzites and shales are more prone to layer-parallel shear than either the lavas or the VCR conglomerates. The major mechanical interface may in these circumstances lie beneath the reef, such that shear strains and associated thrusting are focused into the reef's footwall. In contrast, a massive quartzitic footwall to the VCR provides good mechanical coupling to the lavas through the more deformable VCR, and hence focuses all of the fault–fracture strain within the reef (e.g. Fig. 7a; Jolley et al., 1999, fig. 3). Local facies variation within the VCR, such as quartzite beds and/or channel features, form relatively less-competent bands within the conglomerates, and therefore focus otherwise broad shear strains within the reef (e.g. Fig. 7b). Variation of top and basal VCR landform palaeo-topography and early fault scarp features can be considered as rugosity on the interface between the rigid lavas and the Central Rand Group sediments. These features influence the propagation and geometry of mesoscale thrusts and fractures, and produce additional fracture networks by generating local buttressing strains (e.g. Fig. 7c), and local dilation sites across the contact. Where the reef is thin to non-existent (along low- to non-depositional or erosional inter-terrace slopes) and where the reef is sandy rather than conglomeratic, discrete layer-parallel shear occurs rather than wider zones of fracture generation. Gold-bearing potential is accordingly reduced.

4.2. Mine-scale and 3D seismic reflection data

Data from underground mapping at Elandsrand and Mponeng was compiled into structural maps of the mines (Fig. 9), and compared with maps of gold grade data for the same areas. In this way, we have been able to verify and quantify the up-scaling of our observations to mine- and seismic-scale discussed here, through examination of large confidential datasets. Although we cannot publish these grade data, we can describe the key features of the striking correlation we have seen between thrusting deformation and gold distribution at the mines as follows. The highest gold grades occur within 250 m of the larger mapped compressional structures at Mponeng, and in zones of imbrication and within 50 m either side of steep lateral fault zones, which partition the imbricates into distinct panels at Elandsrand. At Mponeng, a comparison of the structural domains with the distribution of locally famous 'apple green quartzite' shows a remarkably good match (Fig. 9b). These green quartzites, which are broadly associated with elevated gold grades, were once considered to be a primary depositional marker in the VCR package. However, they owe their spectacular pistachio green colour to Cr-bearing sericitic alteration.

Several 3D seismic surveys have been collected over Mponeng and the regional Western Ultra Deep Levels (WUDLS) area south of the Carletonville mines. The pattern of sub-crops beneath the VCR of various Central Rand stratigraphy has been identified by using base-lavas reflection attributes such as amplitudes and waveform tuning (Gibson et al., 2000). Structures have been picked in the seismic data using conventional and attribute-based techniques, and then characterised as thrusts, flexures and normal faults where seismic resolution allows. Thrusts seen in the seismic data to detach from the Booysens Shale and link into the base of the lavas have been correlated with mineralised imbricate zones within an overlap area between the 3D seismic data, and the mine plans and active workings (Jolley et al., 1999; Gibson et al., 2000). At Mponeng, it has been possible to directly compare seismically mapped structures with those observed underground, since extensive mining and geological mapping has taken place in the years following acquisition of a pilot 3D seismic survey there. With such detailed integration work, we are confident that we have been able to map the regional distribution of prospective thrust-related structures in the VCR from the seismic data.

4.3. Prospectivity in the WUDLS exploration ground

Our understanding of the various influences on the hydrothermal mineralisation discussed in this paper and elsewhere (Barnicoat et al., 1997; Jolley et al., 1999) has been used to assess the prospectivity of the regional-scale WUDLS 3D seismic survey area. To do this, we compared a qualitative matrix of these controlling factors with the structure map produced from the seismic data. In doing so, we were able to assign prospectivity 'values' to individual structures, in which seismically mapped thrusts and flexures are judged to be equivalent to gold-bearing thrust-fracture systems mapped in the mines. Comparison of seismically mapped structures with mine plan overlays and the extension of mined-out structures shows that our classification procedure is reasonably robust. Thus, whilst the seismic data resolution only allows the general pattern of thrusting to be identified, we have taken this as a proxy for the distribution of prospective imbricate zones. Based on the mapped zones of faulting in Elandsrand and Mponeng, we have been able to estimate the width of structurally controlled high-grade domains and overlay these onto the picked structures to produce a prospectivity map.

The validity of our classification and mapping approach was tested by comparing our prospectivity map with average gold values determined from existing surface boreholes. Borehole intersections within 250 m of seismically defined thrusts and flexures were found to have significantly higher median gold grades than those further away from them. Using a matrix of the prospectivity criteria and structure map outlined above successfully predicts gold value in 70% of the intersections.

5. Structure and mineralisation, Basal Reef, Welkom goldfield

5.1. Matjhabeng mine

The western margin of the Welkom goldfield (Fig. 1) is defined by the main westerly sub-crop of Central Rand Group rocks against the Ventersdorp volcanics. This margin was the focus of thrusting which produced a major syncline and fanning stack of syn-tectonic unconformities during the latter part of the Central Rand (Coward et al., 1995). Matjhabeng mine, situated in the NW of the goldfield, exploits the older Basal Reef package (Figs. 2 and 11). The key to understanding mineralisation here is the observation that the Basal Reef, together with mesoscale thrusts and fractures hosting hydrocarbons and gold (e.g. Fig. 4), is folded post-depositionally, and that this fold is truncated by the intra-Central Rand basal VS5 unconformity (Figs. 2 and 12). Thus, the thrusting and fracturing, which hosts gold and associated alteration is syn-Central Rand, of an age earlier than that described above in association with VCR mineralisation. At the time of their formation, these structures were similar to those described above for the Vaal Reef.

After deposition of the VS5, the major Rheedersdam thrust breached the folded Basal Reef (Fig. 12) and tipped out below the Klipriviersberg lavas. Its later history relative to the lavas is therefore ambiguous here, although to the north seismic data (e.g. Stuart et al., 2000) shows that the same fault zone forms the forethrust component of a passive roof duplex with backthrusts cutting the lowermost Klipriviersberg and driving associated growth in the basal lavas. At Matjhabeng, the Rheedersdam thrust is associated with extensive pyrophyllitic alteration, including the

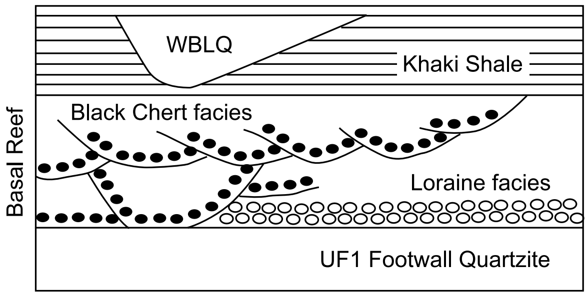

Fig. 11. Stratigraphy enclosing the Basal Reef in the Welkom goldfield. The Khaki Shale (also known as the Booysens Shale) is a layer-cake of 2–6 m thickness: the quartzite wedge it contains is the Waxy Brown Leader Quartzite (WBLQ). The Basal Reef consists of two laterally exclusive conglomeratic packages (the Loraine and Black Chert facies).

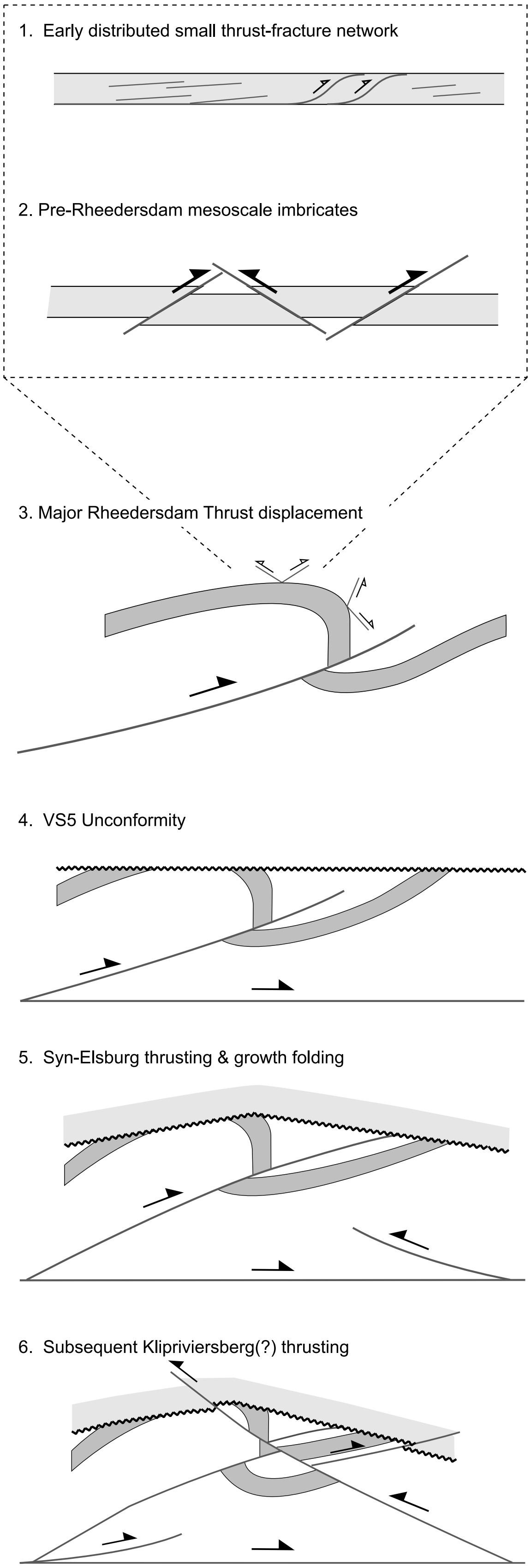

Fig. 12. Cartoon of the late Witwatersrand structural evolution at Matjhabeng mine in the Welkom goldfield.

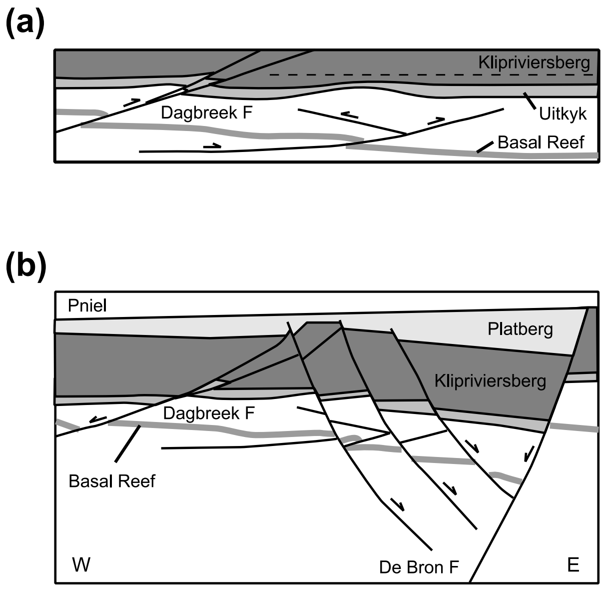

Fig. 13. Sketch sections (based on 3D seismic, underground mapping and borehole data) of the geology at Tshepong mine. (a) During late Central Rand/early Klipriviersberg thrusting. (b) After Platberg extension, including reactivation of earlier thrust faults.

development of veins filled solely with pyrophyllite. This alteration can be clearly seen to overprint earlier alteration associated with the mineralisation.

5.2. Tshepong mine

Tshepong mine, which mainly exploits the Basal Reef (Fig. 11), is situated immediately NE of Matjhabeng in the northern part of the Welkom goldfield. Integration of 3D seismic interpretation, mine plan collation, borehole core logging, underground mapping and SEM petrography, enabled critical structures and events to be determined at Tshepong, which are comparable with the structural evolution of Matjhabeng. The key structural elements necessary for understanding the mineralisation of the Basal Reef at Tshepong are as follows. Numerous early, sub-vertical extensional structures occur in two main orientations: NE/SW and NW/SE. These faults have centimetre-scale offsets, and are either reactivated or cross-cut and decapitated by other suites of structures. They may have originated as 'systematic' fractures and early normal faults typically developed in the foreland ahead of linked thrust fronts (e.g. Hanks et al., 1997; Scisciani et al., 2002). These steep structures are post-dated by low angle low displacement thrusts with NE/SW-trending slickencrysts of quartz and pyrophyllite, and associated distinctive green coloured pyrophyllitic and sulphide alteration. Most of the individual thrusts accommodate very low (centimetre-scale) displacements, and can be seen to exploit and incorporate pre-existing features such as bedding foresets and early steep structures into their fault surfaces. This thrust system comprises a large number of generally unlinked, discontinuous thrusts, which are typically only laterally continuous for a few 10's of metres. Only rarely can a single fault surface be mapped in the stope faces in excess of 50–60 m, although a few larger NW/SE striking frontal structures do occur. Gold grades are significantly elevated by an order of magnitude or more where these features lie in close proximity to the reef. A second suite of thrusts identified at the mine strike NNE/SSW and have a WNW/ESE slip direction, as indicated by elongation of white mica clots formed on associated shear-foliation surfaces. Pyrophyllite–sulphide alteration associated with the earlier generation of thrusts is overprinted by these WNW/ESE verging structures. 3D seismic data clearly shows that uppermost Central Rand stratigraphy and lower Klipriviersberg volcanics thicken and thin across folds formed by these thrusts (Fig. 13a). Post Klipriviersberg extension of Platberg age was accommodated by the development of new faults and by the reactivation of pre-existing thrusts such as the Dagbreek fault, which bisects the mine (Fig. 13b).

6. Orebody model for production planning at Tshepong mine

6.1. Basal Reef stratigraphy and facies variation

The footwall to the Basal Reef at Tshepong mine is a monotonous quartzite package known as the UF1 Footwall Quartzite unit (Fig. 11) The Basal Reef package consists of two conglomeratic facies, the older of which is oligomict with a single basal lag (Loraine facies), while the overlying facies is a multiple scour polymict package (Black Chert facies). The Black Chert facies dominates the reef on the mine, lying directly on the UF1 Quartzite to the south, the diachronous boundary between the two reef facies running NW/SE across the northern part of the mine. These conglomeratic facies are overlain by a 2–6 m thick mudstone–siltstone unit termed the Khaki Shale. The Khaki Shale contains a SE-trending quartzite-filled erosional channel feature, which changes to a quartzite sheet deposited in an outwash plain down depositional dip to the SE (Fig. 14a). The channel-fill and outwash quartzite is termed the Waxy Brown Leader Quartzite (WBLQ).

6.2. Controls on gold distribution

We have mapped underground in transects between low- and high-grade gold mineralisation in detail. This mapping showed that elevated gold grades were consistently associated with pyrophyllite–sericite bearing low displacement thrusts that pass from the underlying quartzites into the conglomeratic reef package or from the overlying quartzites or shale down into the conglomerates. In detail, high gold grades are associated with individual thrusts within the reef package, but diminish where a given structure passes into

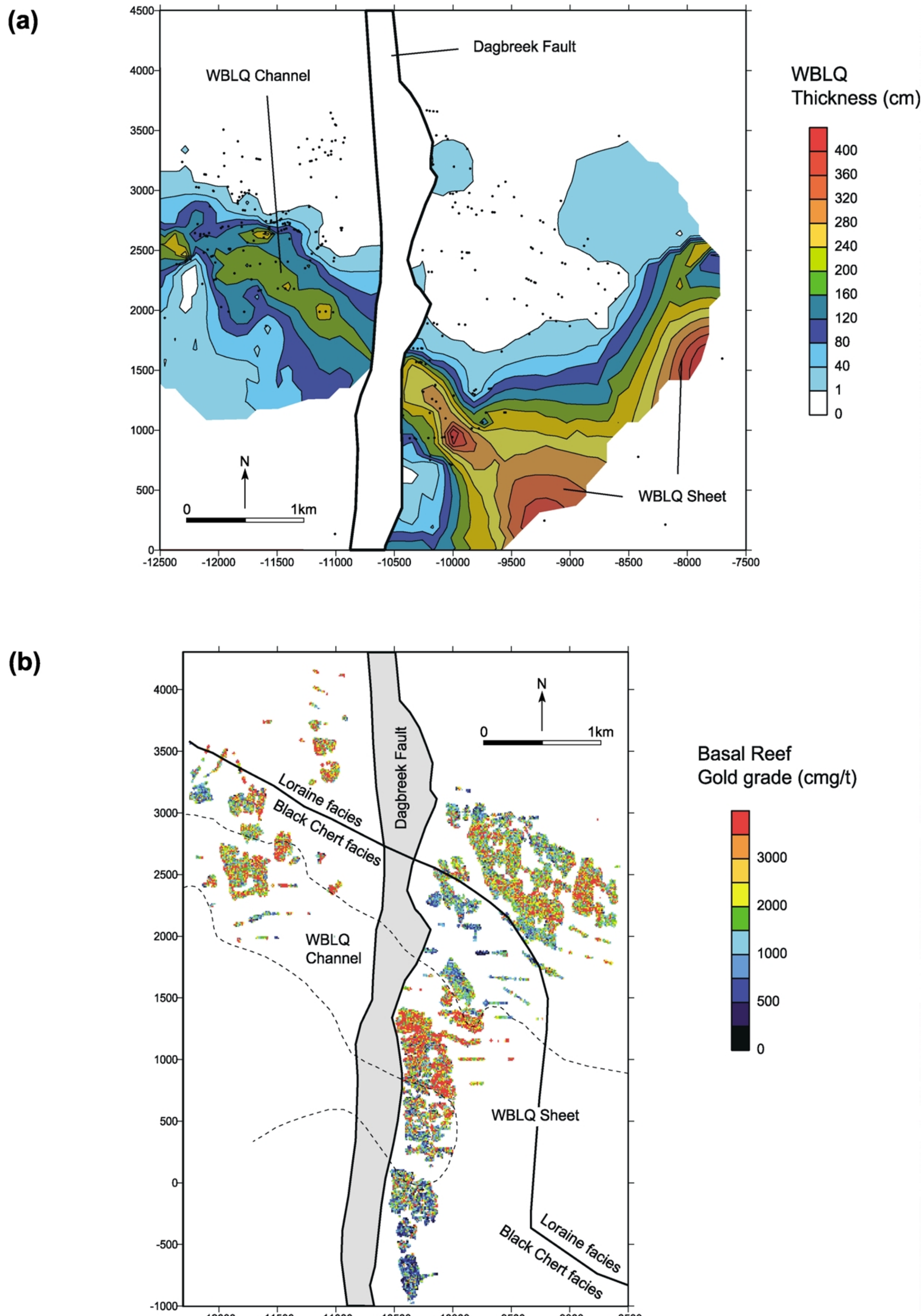
(a)
Dagbreek Fault
WBLQ Channel
WBLQ Sheet
N
0
1km
WBLQ
Thickness (cm)
400
360
320
280
240
200
160
120
80
40
1
0
4500
4000
3500
3000
2500
2000
1500
1000
500
0
-12500
-12000
-11500
-11000
-10500
-10000
-9500
-9000
-8500
-8000
-7500
(b)
Dagbreek Fault
Loraine facies
Black Chert facies
WBLQ Channel
WBLQ Sheet
Loraine facies
Black Chert facies
N
0
1km
Basal Reef
Gold grade (cmg/t)
3000
2000
1000
500
0
4000
3500
3000
2500
2000
1500
1000
500
0
-500
-1000
-12000
-11500
-11000
-10500
-10000
-9500
-9000
-8500

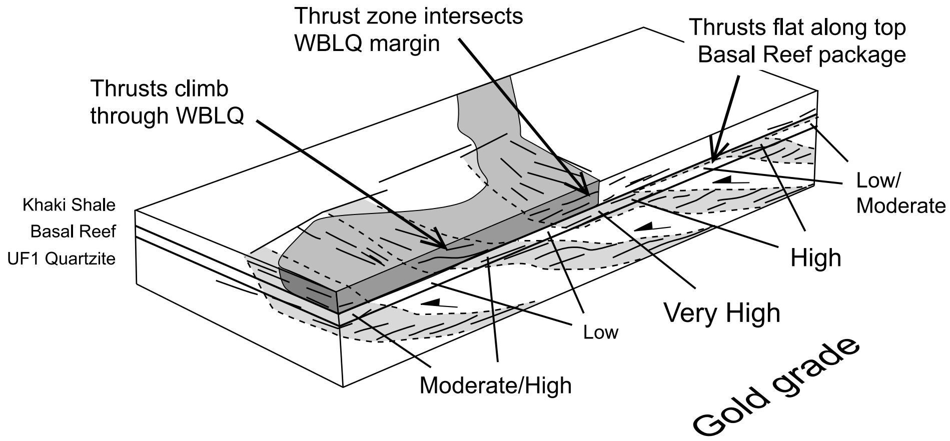

Fig. 15. Summary sketch showing relationships between thrusting and stratigraphy, and associated gold grades at Tshepong mine.

the overlying Khaki Shales or underlying quartzites. Elevated grades were also observed in steep buttressing zones or lateral structures associated with the mineralised thrusts. These steep features appear to be related to the early-formed small (always less than 0.5 m throw), steep oblique extensional structures that developed prior to the main thrusting deformation, possibly as 'systematic' fractures and normal faults within the foreland, ahead of the advancing thrust front. Where the thrust propagation direction was at a high angle to the strike of these steep structures, the interaction caused reverse reactivation, buttressing and fracturing, and hence local gold concentration. Where the propagation direction was close to the strike of the steep structures, they became reactivated and captured by the thrust system as lateral ramps. Therefore, whilst the steep structures control local gold grade, the dominant volumetric control on gold mineralisation is the presence and intensity of the fracturing associated with the mineralised thrust system. The architecture of the thrust–fracture networks and hence the ore-scale gold grade, is controlled by a number of other factors that relate to the mechanical properties of the stratigraphy.

Fig. 14b, shows the distribution of gold at Tshepong superimposed on the location of the Basal Reef facies type boundaries and the distribution of quartzite-filled channel in the Khaki Shale (WBLQ unit). There is a strong correlation between the presence of oligomict, clast-supported conglomerate (Loraine facies) and gold grade. Black Chert facies conglomerates of the Basal Reef contain lower average gold grades than the Loraine facies. Gold grades are also markedly higher in the Basal Reef where it is overlain by the WBLQ channel feature, and especially high beneath the margins of the channel. The tabular outwash area of WBLQ, located in the eastern part of the mine, is a low grade area in which gold content of the reef increases towards the margins of the quartzite body. A further important observation from detailed analysis of the grade data for the mine is the presence of higher-grade lineaments within the data that coincide with areas in which mapped NW/SE striking thrusts intersect the reef package.

Our SEM work on Basal Reef samples from Tshepong shows gold to be hosted within fractures and other secondary, post-diagenetic microstructural sites, most often in association with hydrocarbon mesophase ('carbon') or sulphides, in common with other Witwatersrand reefs. Fractures associated with both steep and flat-lying faults are mineralised in the reef, whilst additional small amounts of gold occur in association with thrust-reactivated steep structures in the footwall. The main controls on the distribution of this syn-kinematic permeability (and therefore gold) are the location of thrusts and variations in the mechanical stratigraphy through which they propagated. For example, clast-supported oligomict conglomerates such as the Loraine facies are more fracture-prone than polymict varieties such as the Black Chert facies. However, the most critical variation in stratigraphy at Tshepong is the distribution of the WBLQ, which removes almost all of the Khaki Shale above the Basal Reef in a SE-trending channel. Variation in WBLQ morphology resulted in variation of the mechanical coupling between stratigraphic elements and propagating thrusts, to affect the distribution of associated mineralised fracture systems within the reef (as summarised in Fig. 15). The fault–fracture network is better developed in the reef where the imbricates climb through it. The areas with the most intense fracture permeability lie beneath the WBLQ channel margins,

Fig. 14. Maps showing Basal Reef attributes at Tshepong mine. Facies and isopachs compiled from logging core from 100 + boreholes. The N–S polygon in the centre of the maps is the locally famous Dagbreek fault zone. (a) Isopach map of the Waxy Brown Leader Quartzite (WBLQ). (b) Gold grade at the mine (kriged to 20 m blocks). Basal Reef facies boundary, WBLQ channel and outwash sheet are indicated. Note better grades associated with the fracture-prone Loraine facies, the sharp increase in grade in the Basal Reef beneath the edge of WBLQ channel, and NW–SE high grade linears in the data (the latter coincide with the mapped trace of thrusts intersecting the reef).

Table 2
Prospectivity matrices for the Basal Reef at Tshepong

		Imbricate thrust zone		
		Intense	Normal	Absent
Loraine facies				
Waxy Brown Leader Quartzite	Channel	10	8	4
	Absent	6	4	2
	Sheet	6?	4	2
Black Chert facies present				
Waxy Brown Leader Quartzite	Channel	8	6	3
	Absent	5	3	1
	Sheet	5?	3	1

where thrusts propagating through the shales above the reef are impeded by interaction with the mechanically more competent quartzites, thus inducing widespread fracturing in the reef package. This effect is exaggerated where it coincides with imbricate thrusts climbing through the reef. However, where thrusts climb through the reef package where it is overlain by shales, the faults detach within the shales and follow the contact, thus limiting the fracture strains in the reef. When there is no shale above the reef (e.g. where this is replaced by the WBLQ outwash sheet), there is little lithological variation to interrupt fault propagation across the contact. The thrusts therefore continue to climb as relatively discrete structures through the stratigraphy, inducing only modest subsidiary fracturing in the reef package.

6.3. Application of orebody model

Key parameters that control gold distribution in the Basal Reef at Tshepong are thus: the location of the thrust imbricate zones; the presence and form of the WBLQ in the hanging wall to the Basal Reef; and the Basal Reef facies type. A qualitative matrix can therefore be used to rank differing combinations of these parameters for geological assessment of reef pay for production planning and near-facilities exploration, based upon a visual inspection of the correlation between gold grade and parameter combination (Table 2). Detailed statistical analysis of the relationships between these parameters and gold grades bear out these qualitative assessments (summarised in Fig. 16). Furthermore, recent drilling on the basis of this guidance at Tshepong has proved successful, and influenced further production planning and economic assessment accordingly.

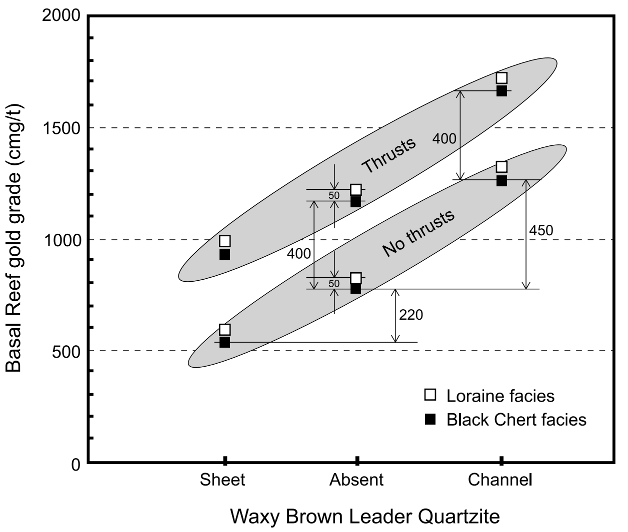

Fig. 16. Basal Reef gold grade values at Tshepong mine estimated by multiple regression of sampling data using the key parameters outlined in the text. Each summary data point shown here is based on several thousands of individual data points. Note the consistent differences between areas with and without thrusting, WBLQ channel, sheet or absence, and between the different Basal Reef facies.

7. Discussion

The gross distribution of lithological units in the Witwatersrand has been re-organised into blocks bounded between Platberg graben forming normal faults. However, previous workers (e.g. Myers et al., 1990; Coward et al., 1995) have clearly documented significant earlier thrusting along the northern and western margins of the basin. It is this earlier, thrust-related deformation that we consider critical to gold mineralisation and distribution. Our observations show that mineralisation was post-diagenetic, indicating that sedimentary permeability was effectively closed, and as discussed here and elsewhere (Barnicoat et al., 1997; Jolley et al., 1999; Phillips and Law, 2000), initially sub-horizontal shear zones/faults (marked by phyllonites and cataclasites) mark the sites of extensive hydrothermal fluid flow and alteration, and are linked to the generation of fractures that host almost all of the gold, uraninite and hydrocarbons in the Witwatersrand basin. The mechanical influence of stratigraphy on development of fault geometry, size and frequency distribution is well documented in the literature (e.g. Woodward, 1992; Couzens and Wiltschko, 1996; Gross et al., 1997; Hanks et al., 1997; Cook and MacLean, 1999; Wilkins and Gross, 2002). In the Witwatersrand Basin, the mechanical properties of

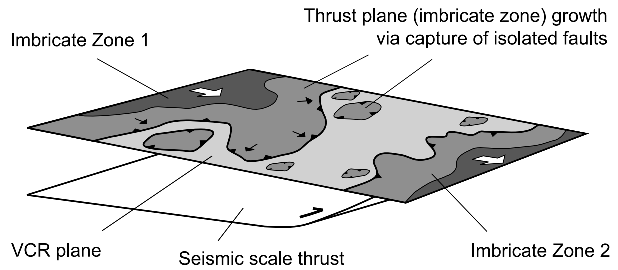

Fig. 17. Cartoon of the front of a propagating thrust imbricate zone (cf. Fig. 9). Isolated patches of faulting occur in advance of the tip line to the main imbrication, which grows by coalescing these isolated slip patches. Frontal and lateral ramps and footwall plucking structures develop to facilitate capture of slip patches ahead and above or below the main tip line, respectively.

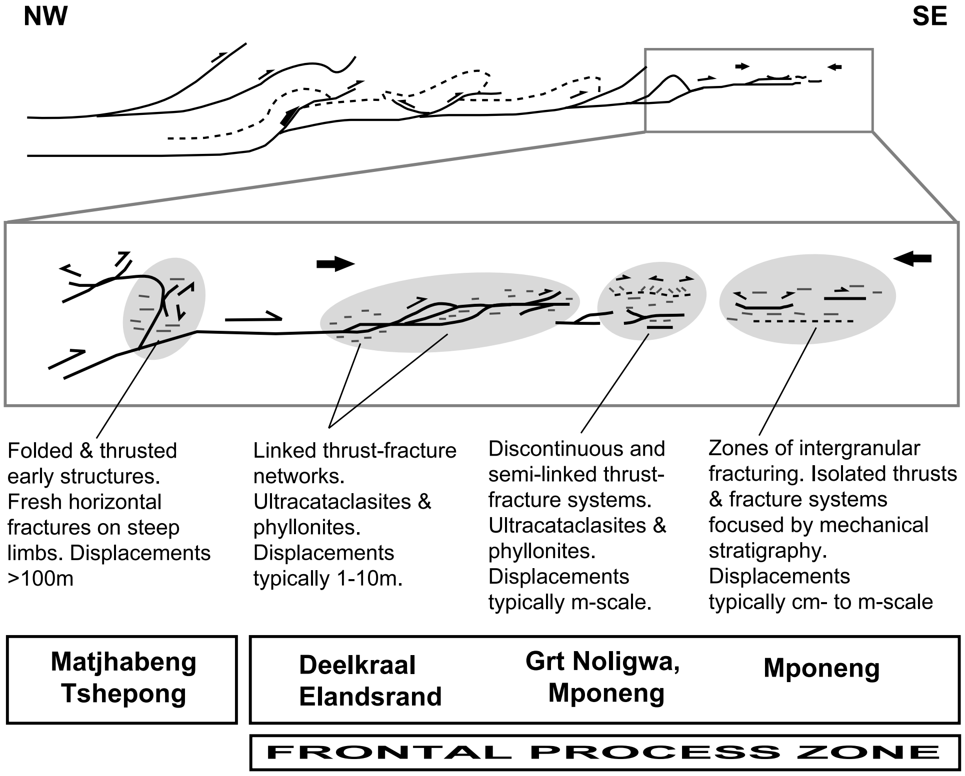

Fig. 18. Schematic thrust system, showing the styles of structures seen within the frontal process zone. Note the setting of various Witwatersrand mines. The structural history described for the mines in the text is compatible with progressive diachronous deformation in a thrust system with early formed, low displacement structures becoming folded and cut by thrusts upon arrival of the propagating imbricate system.

stratigraphy are seen to have exerted controls on development of the mineralised thrust–fracture network at macro- to micro-scales of observation. Examples described here include the kilometre-scale strain discontinuity between the rigid Klipriviersberg and the less competent Central Rand groups, accommodated by decoupling across thrust–fracture systems within the VCR; and the macro- to meso-scale variation of efficiency in mechanical coupling between stratigraphic elements, caused by variations in the distribution of quartzites, conglomerates, shales and bedforms within Basal Reef and VCR depositional packages. Conglomeratic units are fracture-prone with respect to finer grained lithologies, and therefore tend to host the better-developed mineralised fault–fracture arrays in multilayers subjected to thrusting deformation, whilst the adjacent quartzites generally remain barren. This general association between stratigraphy and gold has in the past led to syngenetic interpretations. However, as described in this paper, economic concentration of gold is controlled by development of mineralised thrust–fracture arrays, through the interplay between thrusting deformation and the stratigraphic template.

Thrusting in the Witwatersrand gold mines generally forms low displacement (centimetre–metre scale) systems, which we interpret as representing a typical frontal process zone to a thrust belt, where the isolated and partially linked thrust and fracture networks are developed on the foreland side of the mapped sole thrust. In such sites, areas of small amounts of slip occur in advance of the linked imbrication front, and their capture facilitates the advance of the main thrust system (Fig. 17). Fig. 18 is a schematic section based on our seismic interpretations and observations in the mines, showing the variation in structural styles and progressive strain evolution seen in a thrust system's low-displacement, frontal process zone. Viewed in terms of hydrothermal 'plumbing', the larger structures within the linked thrust system would form upstream flow backbones growing from the hinterland, and the smaller semi-linked mesoscale thrust–fracture networks, would represent smaller-scale 'dangling' elements facilitating downstream hydrothermal discharge, an arrangement seen in other mesothermal mineralising systems (e.g. Cox, 1999). It is clear from the observations and interpretations presented in this paper that careful synthesis of integrated work across scales from that of thin sections to that of the whole basin, is essential to the development of a fuller understanding of ore-forming processes in the Witwatersrand, and the generation of effective process-based exploration–production models.

Acknowledgements

This paper is drawn from over a decade of our work in the Witwatersrand Basin, principally under contract to

Anglo-American and subsequently AngloGold, to whom we are grateful for the opportunity and financial support. We are grateful to the many geoscientists and engineers we have interacted with working on Witwatersrand mines; discussions with them and with John Walshe, Bruce Hobbs, Dave Kershaw and Mark Gibson have helped to shape our ideas. We are grateful to AngloGold for permission to publish this work, and to Shell for funding to reproduce figures in colour. Constructive comments from reviewers Johnathan Law, Richard Spencer and Julian Vearncombe helped to improve our manuscript.

References

Barnicoat, A.C., Henderson, I.H.C., Knipe, R.J., Yardley, B.W.D., Napier, R.W., Fox, N.P.C., Kenyon, A.K., Muntingh, D.J., Strydom, D., Winkler, K.S., Lawrence, S.R., Cornford, C., 1997. Hydrothermal gold in the Witwatersrand Basin. Nature 386, 820–824.

Barnicoat, A.C., Yardley, B.W.D., Henderson, I.H.C., Fox, N.P.C., 1999. Discussion of 'Detrital origin of hydrothermal gold' by H.E. Frimmel. Terra Nova 10, 347–349.

Barnicoat, A.C., Phillips, G.M., Law, J.D.M., Walshe, J.L., Phillips, G.N., Fox, N.P.C., 2000. Refuting the irrefutable: a new look at a well-known sample of Witwatersrand gold mineralisation. Economic Geology Research Unit James Cook University, Contribution 59, 16–17.

Berlenbach, J.W., 1995. Underthrusting in the Kloof Gold Mine. South African Journal of Geology 98, 35–42.

Cook, D.G., MacLean, B.C., 1999. The Imperial anticline, a fault–bend fold above a bedding-parallel thrust ramp, Northwest Territories, Canada. Journal of Structural Geology 21, 215–228.

Couzens, B.A., Wiltschko, D.V., 1996. The control of mechanical stratigraphy on the formation of triangle zones. Bulletin of Canadian Petroleum Geology 44, 165–179.

Coward, M.P., Spencer, R.M., Spencer, C.E., 1995. Development of the Witwatersrand Basin, South Africa. In: Coward, M.P., Ries, A.C. (Eds.), Early Precambrian Processes. Geological Society, London, Special Publications 95, pp. 243–269.

Cox, S.F., 1999. Deformational controls on the dynamics of fluid flow in mesothermal gold systems. In: McCaffrey, K.J.W., Lonergan, L., Wilkinson, J.J. (Eds.), Fractures, Fluid Flow and Mineralization. Geological Society, London, Special Publications 155, pp. 123–140.

England, G.L., Rasmussen, B., Krapež, B., Groves, D.I., 2001. The origin of uraninite, bitumen nodule, and carbon seams in Witwatersrand gold–uranium–pyrite ore deposits, based on a Permo-Triassic analogue. Economic Geology 96, 1907–1920.

Feather, C., Koen, G.M., 1975. The mineralogy of the Witwatersrand reefs. Minerals Science and Engineering 7, 189–224.

Fox, N.P.C., 2002. Exploration for Witwatersrand deposits and analogues. In: Cooke, D.R., Pongratz, J. (Eds.), Giant Ore Deposits: Characteristics, Genesis and Exploration. CODES Special Publication 4, 243–269.

Frimmel, H.E., Minter, W.E.L., 2002. Recent developments concerning the geological history and genesis of the Witwatersrand gold deposits, South Africa. Society of Economic Geologists, Special Publication 9, 17–45.

Germs, G.J.B., Schweitzer, J.K., 1994. A provisional model for the regional morphostratigraphy of the Venterspost Conglomerate Formation in the West Rand and Carletonville goldfields. South African Journal of Geology 97, 279–287.

Gibson, M.A.S., Jolley, S.J., Barnicoat, A.C., 2000. Interpretation of the Western Ultra Deep Levels 3D seismic survey. The Leading Edge 19, 730–735.

Gize, A.P., 2000. Organic petrology applied to ore deposits. Reviews in Economic Geology 9, 63–85.

Gray, G.J., Lawrence, S.R., Kenyon, K., Cornford, C., 1998. Nature and origin of carbon in the Archean Witwatersrand basin, South Africa. Journal of the Geological Society, London 155, 39–59.

Gross, M.R., Gutierrez-Alonso, G., Bai, T., Wacker, M.A., Collinsworth, K.B., 1997. Influence of mechanical stratigraphy and kinematics on fault scaling relations. Journal of Structural Geology 19, 171–183.

Hall, R.C.B., 1994. Supporting evidence for the placement of the inter-reef lavas and associated sediments within the Venterspost Conglomerate Formation: Kloof Gold Mine. South African Journal of Geology 97, 297–307.

Hanks, C.L., Lorenz, J., Tuefel, L., Krumhardt, A.P., 1997. Lithologic and structural controls on natural fracture distribution and behaviour within the Lisburne Group, northeastern Brooks Range and North Slope subsurface, Alaska. AAPG Bulletin 81, 1700–1720.

Henning, L.T., Els, B.G., Mayer, J.J., 1994. The Ventersdorp Contact Placer at Western Deep Levels South Gold Mine—an ancient terraced fluvial system. South African Journal of Geology 97, 308–318.

Jolley, S.J., Henderson, I.H.C., Barnicoat, A.C., Fox, N.P.C., 1999. Thrust-fracture network and hydrothermal gold mineralisation: Witwatersrand Basin, South Africa. In: McCaffrey, K.J.W., Lonergan, L., Wilkinson, J.J. (Eds.), Fractures, Fluid Flow and Mineralization. Geological Society, London, Special Publications 155, pp. 153–165.

Lavery, R.K., 1989. The effect of flat faulting on the Ventersdorp Contact Reef on Elandsrand Gold Mine. Anglo American Corporation Occasional Report.

McWha, M., 1994. The influence of landscape on the Ventersdorp Contact Reef at Western Deep Levels South Mine. South African Journal of Geology 97, 319–331.

Minter, W.E.L., 1999. Irrefutable detrital origin of Witwatersrand gold and evidence of eolian signatures. Economic Geology 94, 665–670.

Myers, R.E., McCarthy, T.S., Stanistreet, I.G., 1990. A tectono-sedimentary reconstruction of the development and evolution of the Witwatersrand basin, with particular emphasis on the Central Rand Group. South African Journal of Geology 93, 180–201.

Palmer, J.A., Phillips, G.N., McCarthy, T.S., 1989. Paleosols and their relevance of Precambrian atmospheric composition. Journal of Geology 97, 77–92.also 764–766.

Parnell, J., 1996. Phanerozoic analogues for carbonaceous matter in Witwatersrand ore deposits. Economic Geology 91, 55–62.

Phillips, G.N., 1987. Metamorphism of the Witwatersrand goldfields: conditions during peak metamorphism. Journal of Metamorphic Geology 5, 307–322.

Phillips, G.N., Law, J.D.M., 2000. Witwatersrand gold fields: geology, genesis and exploration. Reviews in Economic Geology 13, 439–500.

Phillips, G.N., Myers, R.E., 1989. Witwatersrand goldfields: Part II: an origin for Witwatersrand gold during metamorphism and associated alteration. Economic Geology Monograph 6, 598–608.

Scisciani, V., Tavarnelli, E., Calamita, F., 2002. The interaction of extensional and contractional deformations in the outer zones of the Central Appenines, Italy. Journal of Structural Geology 24, 1647–1658.

Stuart, G.W., Jolley, S.J., Polome, L.G.B.T., Tucker, R.F., 2000. Application of 3-D seismic attributes analysis to mine planning: Target gold deposit, South Africa. The Leading Edge 19, 736–742.

Wilkins, S.J., Gross, M.R., 2002. Normal fault growth in layered rocks at Split Mountain, Utah: influence of mechanical stratigraphy on dip linkage, fault restriction and fault scaling. Journal of Structural Geology 24, 1413–1429.

Woodward, N.B., 1992. Deformation styles and geometric evolution of some Idaho–Wyoming thrust belt structures. In: Mitra, S., Fisher, G.W. (Eds.), Structural Geology of Fold and Thrust Belts, Johns Hopkins University Press, Baltimore, pp. 191–206.